




## ORIGINAL ARTICLE OPEN ACCESS

# Clinico-Pathological Significance of Tumor Infiltrating Immune Cells in Oral Squamous Cell Carcinoma—Hope or Hype?

Rajkumar K. Seenivasagam<sup>1,2</sup> | Ashok Singh<sup>3</sup> | Vinay N. Gowda<sup>3,4</sup> | Dharma R. Poonia<sup>2,5</sup>  | Kinjal S. Majumdar<sup>2,6,7,8</sup>  | Thaduri Abhinav<sup>2,8,9</sup>  | Pallvi Kaul<sup>2,8,10</sup> | Achyuth Panuganti<sup>2,8,11</sup> | Vikramjit S. Kailey<sup>8,12</sup> | Rahul Kumar<sup>2</sup> | Nilotpal Chowdhury<sup>3</sup>

<sup>1</sup>Department of Surgical Oncology, PSG Institute of Medical Sciences & Research, Coimbatore, India | <sup>2</sup>Department of Surgical Oncology, All India Institute of Medical Sciences, Rishikesh, India | <sup>3</sup>Department of Pathology, All India Institute of Medical Sciences, Rishikesh, India | <sup>4</sup>Department of Pathology and Laboratory Medicine, All India Institute of Medical Sciences, Jodhpur, India | <sup>5</sup>Department of Surgical Oncology, All India Institute of Medical Sciences, Jodhpur, India | <sup>6</sup>Department of Head & Neck Surgery, Kasturba Medical College, Manipal, India | <sup>7</sup>Manipal Academy of Higher Education, Manipal, India | <sup>8</sup>Department of Otolaryngology—Head & Neck Surgery, All India Institute of Medical Sciences, Rishikesh, India | <sup>9</sup>Department of ENT, Prathima Relief Institute of Medical Sciences, Warangal, India | <sup>10</sup>Department of Surgical Oncology, Shri Guru Ram Rai Institute of Medical and Health Sciences, Dehradun, India | <sup>11</sup>Department of ENT, Medicit Institute of Medical Sciences, Medchal, India | <sup>12</sup>Mohandai Oswal Hospital, Ludhiana, India

**Correspondence:** Kinjal S. Majumdar ([kinjal.majumdar@manipal.edu](mailto:kinjal.majumdar@manipal.edu); [drkinjalmajumdar@gmail.com](mailto:drkinjalmajumdar@gmail.com))

**Received:** 20 August 2024 | **Revised:** 29 November 2024 | **Accepted:** 12 January 2025

**Funding:** This work was supported by All India Institute of Medical Sciences, Rishikesh, India under Intra-mural Grant (AIIMS/IM/RC/163/2020/8) and Manipal Academy of Higher Education.

**Keywords:** Oral cancer | squamous cell carcinoma | tumor-associated macrophages | tumor-infiltrating lymphocytes | tumor microenvironment

## ABSTRACT

**Background:** To correlate between immunohistochemical expression of tumor-infiltrating lymphocytes (TILs), tumor-associated macrophages (TAMs), and natural killer (NK) cells with the AJCC 8th edition TNM staging system and other disease-modifying clinico-pathological variables.

**Methods:** The representative histology sections of tumor invasive margin (IM) and tumor core (TC) were selected according to the International Immuno-Oncology Biomarker Working Group and were subjected to immunohistochemistry with antibodies for TILs (CD3, CD8, FOXP3), NK Cells (CD57), TAMs (CD68, CD163) and pan-leukocyte marker (CD45). Histo-immuno-density-intensity (HIDI) scoring was calculated as a product of the proportion and intensity of staining. Ordinal-ordinal and continuous-ordinal variables were correlated using Kendall's tau-b ( $\tau_b$ ), and binary-ordinal variables were correlated using Rank-Biserial ( $r_{rb}$ ) statistics.

**Results:** A total of 111 patients were included in the study. None of the clinical and pathological parameters showed a strong correlation with any of the immune infiltrates including TNM staging.

**Conclusion:** We hypothesize an independent activity of tumor immunology in the disease prognosis.

**Trial Registration:** CTRI/2020/07/026335

## 1 | Introduction

Over the past two decades, human malignancies have increasingly been recognized as heterogeneously complex tissues rather than merely collections of relatively homogeneous malignant cells [1, 2]. Cells involved in immune response as well as native cells present in the background interstitium are increasingly documented to be functionally important for the disease manifestation. Recent understanding of the involvement of inflammatory cells in disease progression and prognostication has revealed the significance of immuno-characterization of human malignancies [3, 4]. The effect of immune cell infiltration on carcinogenesis varies and is based on the class of immune cells and their spatial differential distribution within the tumor microenvironment (TME), making it a viable proposition for prognostic biomarker study. To quantify the effect of tumor-infiltrating immune cells in disease prognostication, numerous scoring systems have been proposed and validated on varied study populations; few extrapolated from different sites, and the rest indigenously developed. An international consortium has been commenced to validate and promote the “TNM-Immunoscore” for colorectal cancers in routine clinical settings [5, 6]. Similar work is in progress for breast cancers and non-small cell lung cancers as well [7, 8]. Studies evaluating tumor-infiltrating immune cells in head and neck squamous cell carcinoma (HNSCC) have been limited by small cohort sizes, the limited panel of immune infiltrates, retrospective approaches, the inclusion of heterogeneous populations, and discrepant findings. Several factors like the inclusion of multiple head and neck subsites, HPV/p16 status, lack of technical and statistical standardization, and non-adherence to the reporting guidelines might contribute to these differences and hamper direct comparison of the studies reported in the literature [9–11].

The present study is designed to evaluate the full spectrum of tumor immune infiltrates on a relatively homogeneous population of oral squamous cell carcinoma (OSCC). The objective was to correlate the differential expression of tumor-infiltrating lymphocytes (TILs), tumor-associated macrophages (TAMs), and natural killer (NK) cells through a semiquantitative scoring with the TNM classification and other proven disease-modifying clinical and pathological variables.

## 2 | Materials and Methods

### 2.1 | Study Design and Participants

In this prospective observational study, all patients with biopsy-proven OSCC of stage I–IV, Eastern Cooperative Oncology Group Performance Status (ECOG PS) 0–2, who underwent curative surgical excision at a tertiary-level healthcare academic institute from July 2020 to December 2021 were included. Patients who operated for residual or recurrent disease, presence of synchronous malignancy, and previous administration of systemic therapy and/or radiotherapy were excluded. The study was in accordance with the guidelines set by the Declaration of Helsinki, and the International Council for Harmonization—Good Clinical Practice. Prior approval was obtained from the Institutional Ethics Committee (AIIMS/IEC/20/409). The

trial is registered under the Clinical Trials Registry—India (CTRI/2020/07/026335). This work was supported by the All India Institute of Medical Sciences, Rishikesh, India under an Intra-mural Grant [AIIMS/IM/RC/163/2020/8].

Informed consent was obtained from each study participant before enrolment, and treatment was delivered in compliance with the standard guidelines. The tumors were staged according to the American Joint Committee on Cancer/Union for International Cancer Control (AJCC/UICC) 8th edition TNM classification system [12]. Recommendations by the National Cancer Institute—European Organization for Research and Treatment of Cancer (NCI-EORTC) Working Group on Cancer Diagnostics (REMARK) were followed for reporting [13].

### 2.2 | Histopathology and Immunohistochemistry

After submission of the specimen, the histology sections of the primary specimen representative of tumor invasive margin (IM) and tumor core (TC) were selected (magnification 200–400x) after initial screening under microscope at low power field (100x) by a single oncopathologist (AS) according to the recommendations by the International Immuno-Oncology Biomarker Working Group (IIOB-WG) [14]. Respective formalin-fixed paraffin-embedded (FFPE) blocks were acquired from the departmental tissue repository. Fresh tissue sections of 4  $\mu$ m thickness were obtained on AutoFrost Adhesion Microscope Slides (Cancer Diagnostics Inc., NC, USA). All the steps of IHC were performed strictly as per instructions given in the manufacturer-provided information booklets. IHC for positive control/ negative controls was performed on lymph node sections prior to each batch.

The slides were placed in the incubator at 70°C followed by two washes of Tinto Deparaffinator (Bio SB, CA, USA). Tissue rehydration was achieved with graded ethyl alcohol (100%, 90% and 70%, successively) to water. Epitope retrieval was performed using an Immuno/DNA Retriever with EDTA at pH 7.5 (Bio SB, CA, USA) and Multi Epitope Retrieval System (PathnSitu Biotechnologies, CA, USA). Once tissues were cooled down to room temperature, slides were kept in the moist chambers designed for IHC. Tissues on charged slides were outlined with a reagent-repellent pen and were exposed to PolyDetector Peroxidase Block (Bio SB, CA, USA) for 10 min. After washing with ImmunoDNAWasher (Bio SB, CA, USA), prediluted primary antibodies (Bio SB, CA, USA) for TILs (CD3 rabbit monoclonal antibody i.e., RMaB, CD8 mouse monoclonal antibody i.e., MmaB and FOXP3 RMaB), NK Cells (CD57 MmaB), TAMs (CD68 MmaB, CD163 RMaB) and pan-leukocyte marker (CD45 MmaB) were applied for 60 min followed by a wash with ImmunoDNAWasher. MedaView One-step Polymer-AP Anti-Mouse&Rabbit secondary antibody (Medaysis, CA, USA) was applied for the next 20 min, again followed by a wash with ImmunoDNAWasher.

Lastly, DAB chromogen (dilution 50  $\mu$ L/mL with substrate) was applied for 5 min in each tissue section. The slides were washed in distilled water again and counterstained with Hematoxylin for 2 min. Once excess Hematoxylin was washed under running tap water, tissue dehydration was performed in graded ethyl

alcohol series for 2 min (70%, 90%, 100%, and 100%), followed by immersion in Xylene 2 times, 2 min each and mounting of the coverslip.

### 2.3 | Quantification of IHC

Images of IHC slides were captured using a microscope (Olympus BX53) camera (ProgRes capture SPEEDXT CORE 5) based ProgRes capture pro 2.8.8 Jenoptik optical system at 200X magnification. The invasive margin was defined as a 1 mm wide zone centered on the border of the malignant cells with the host tissue, and the tumor core is defined as the central tumor tissue surrounded by this zone as defined by the IIOB-WG [14]. The area selected for capturing the images was based on the area showing the deepest invasive margin and the corresponding tumor core areas, out of which the best areas were selected solely at the discretion of the concerned oncopathologist (AS). Semiquantitative histo-immuno-density-intensity (HIDI) score was calculated as a product of the proportion of area stained and intensity of staining as follows: (0) no stain; (1) 0%–10%, mild intensity; (2) 11%–75%, intermediate intensity; (3) 76%–100%, strong intensity; and ranged from 0 to 9 (weakest to strongest). The scoring was performed separately by two oncopathologists (AS and VN). Any discordance was discussed between the co-authors and resolved by consensus involving a third oncopathologist (NC).

### 2.4 | Data Definition and Categorization

The variables were categorized as mentioned: depth of invasion [12] (DOI) as  $\leq 5$ ,  $> 5$  mm/ $\leq 10$  mm, and  $> 10$  mm; extranodal extension [12] (ENE) as absent, ENEmi ( $< 2$  mm), and ENEm (2 mm); and worst pattern of invasion (WPOI) as WPOI 1–4 and WPOI 5. Lymphovascular invasion (LVI) and perineural invasion (PNI) were classified as absent and present. The lymph node ratio (LNR) is defined as the number of positive nodes divided by lymph nodal yield. The total number of positive lymph nodes and lymph node ratio (LNR) were further categorized into three subgroups according to a previously published study (Table 1) [15].

### 2.5 | Statistical Analyses

The statistical analysis was performed using IBM SPSS statistics version 26 for Windows. Bivariate correlations were performed between individual HIDI score (ordinal) and the nominal (subsite), ordinal (cT, cN, pT, and pN classifications, clinical and pathological stages, histological grade, DOI, ENE), binary (LVI, PNI, WPOI, level-IV/V metastases, contralateral nodal metastases) and continuous (total positive lymph nodes, and LNR) variables. Pearson's chi-square statistic was used for measuring associations between subsite and HIDI score. Ordinal-ordinal and continuous-ordinal variables were correlated using Kendall's tau-b ( $\tau_b$ ), and binary-ordinal variables were correlated using Rank-Biserial ( $r_{rb}$ ) statistics. The association between subsites and HIDI score was determined using Pearson's chi-square statistic. A P-value less than 0.05 was considered statistically significant.

## 3 | Results

One hundred and fifty-six ( $n = 156$ ) patients with OSCC matched the inclusion criteria. Forty-five ( $n = 45$ ) patients were excluded because of neoadjuvant chemotherapy i.e., NACT ( $n = 18$ ), residual or recurrent disease with or without prior radiotherapy and/or systemic therapy ( $n = 16$ ), final histopathology suggestive of non-SCC primary including verrucous carcinoma ( $n = 6$ ), denial or unfit for surgery ( $n = 4$ ), and synchronous breast malignancy ( $n = 1$ ). One hundred and eleven ( $n = 111$ ) patients were included in the study (Figure 1).

Mean age at presentation was 47.7 ( $\pm 11.3$ ) years with male predominance (91%). The majority of them were exposed to tobacco; more to smokeless (72.9%) than smoking forms (49.5%). Buccal mucosa and retromolar trigone were the most common primary subsites (55%) followed by the oral tongue (26.1%). The majority of them presented at a locally advanced stage (cT3/4—79.3%; cN2/3—52.2%; stage III/IV—85.6%). The basic characteristics of the study cohort are highlighted in Table 1.

CD3<sup>+</sup> and CD8<sup>+</sup> TILs and CD168<sup>+</sup> TAMs have shown a strong tumoral infiltration. On the contrary, poor immune infiltration was demonstrated by FOXP3<sup>+</sup> TILs and CD57<sup>+</sup> NK cells across the study cohort. The distribution of HIDI scores across various tumor immune infiltrates is given in Table 2.

Individual HIDI score was higher in the invasive margin than tumor core across all immune infiltrates. A strong positive correlation was found between IM and TC compartments for each of the immune infiltrates except CD45<sup>+</sup> leukocytes. However, spatial distribution and HIDI score did not correlate strongly between two different infiltrating immune cells (Table 3). The density and distribution of immune infiltrates in the TME are shown in Figure 2.

None of the clinical and pathological parameters showed a strong correlation with any of the immune infiltrates including T/N classifications and AJCC/UICC staging system for OSCC. The strongest correlation noticed in the study cohort was between ENE and CD57-TC score ( $\tau_b = 0.266$ ;  $p = 0.03$ ) followed by cN classification and CD68-TC score ( $\tau_b = 0.212$ ;  $p = 0.006$ ). Pathological bone invasion demonstrated a weak-to-moderate negative correlation with the pan-leukocyte marker CD45 in the invasive margin only ( $r_{rb} = -0.351$ ;  $p = 0.002$ ). There were no significant associations between subsites and HIDI score too. The correlation statistics are briefed in Table 4 and detailed in Table S1.

We conducted a post hoc analysis to examine whether the addition of intensity of staining to density has altered the correlations when compared to density-only scoring as proposed by the IIOB-WG. The density-only scoring was according to the present study methodology (range 0–3) and showed minimal variation from the HIDI score (Table S2). The second post hoc analysis was performed by clubbing the HIDI score range from 0–9 to 1–3 (1 = HIDI 0–3, absent or minimal immune infiltration; 2 = HIDI 4–6, moderate immune infiltration; 3 = HIDI 7–9; high immune infiltration); which also turned out to be non-contributory for the major clinical and pathological variables (Table S3).

**TABLE 1** | Basic characteristics of the study participants (*n* = 111).

Characteristics	Number (%)	Characteristics	Number (%)
Age at presentation		Depth of invasion	
≤40years	32 (28.8%)	≤ 5 mm	16 (19.1%)
41–60years	63 (56.8%)	> 5 mm, ≤ 10 mm	21 (21.4%)
> 60years	16 (14.4%)	> 10 mm	74 (56.9%)
Sex		Worst pattern of invasion	
Male	101 (91%)	1–4	88 (79.3%)
Female	10 (9%)	5	23 (20.7%)
Smokeless tobacco		Bone invasion	
Current	36 (32.4%)	Present	25 (22.5%)
Former	45 (40.5%)	Absent	52 (46.8%)
Never	30 (27%)	Not applicable	34 (30.6%)
Smoking		Lymphovascular invasion	
Current	28 (25.2%)	Present	15 (13.5%)
Former	27 (24.3%)	Absent	96 (86.5%)
Never	56 (50.5%)		
Alcohol		Perineural invasion	
Current	24 (21.6%)	Present	12 (10.8%)
Former	18 (16.2%)	Absent	99 (89.2%)
Never	69 (62.2%)		
ECOG PS <sup>a</sup>		Total lymph node-positive	
0	14 (12.6%)	0	53 (47.7%)
1	92 (82.9%)	1–2	30 (27%)
2	5 (4.5%)	3–4	16 (14.4%)
		≥ 5	12 (10.8%)
Charlson comorbidity index		Lymph node ratio	
2	58 (52.3%)	0	53 (47.7%)
3	31 (27.9%)	< 0.1	49 (44.1%)
4	16 (14.4%)	0.1–0.4	8 (7.2%)
≥ 5	6 (5.4%)	> 0.4	1 (0.9%)
Subsite		Extranodal extension	
Buccal mucosa & RMT <sup>b</sup>	61 (55%)	ENema	11 (9.9%)
Tongue & FOM <sup>c</sup>	29 (26.1%)	ENEmi	7 (6.3%)
Lower alveolus	10 (9%)	Absent	40 (36%)
Upper alveolus & hard palate	8 (7.2%)	Not applicable (pN0)	53 (47.7%)
Mucosal lip	3 (2.7%)		
cT classification <sup>d</sup>		pT classification <sup>d</sup>	
T1	5 (4.5%)	T1	9 (8.1%)
T2	18 (16.2%)	T2	20 (18%)

(Continues)

TABLE 1 | (Continued)

Characteristics	Number (%)	Characteristics	Number (%)
T3	22 (19.8%)	T3	30 (27%)
T4	66 (59.5%)	T4	52 (47.8%)
cN classification <sup>d</sup>		pN classification <sup>d</sup>	
N0	34 (30.6%)	N0	53 (47.7%)
N1	19 (17.1%)	N1	13 (11.7%)
N2	41 (36.9%)	N2	29 (26.1%)
N3 <sup>e</sup>	17 (15.3%)	N3	16 (14.4%)
Clinical stage <sup>d</sup>		Pathological stage <sup>d</sup>	
I	5 (4.5%)	I	6 (5.4%)
II	11 (9.9%)	II	16 (14.4%)
III	8 (7.2%)	III	18 (16.2%)
IV	87 (78.4%)	IV	71 (64%)
Histological grade		Level IV/V metastases	
Well-differentiated	58 (52.3%)	Present	5 (4.5%)
Moderately differentiated	52 (46.8%)	Absent	41 (36.9%)
Poorly differentiated	1 (0.9%)	Not applicable	65 (58.6%)

<sup>a</sup>ECOG PS, eastern cooperative oncology group performance status.

<sup>b</sup>RMT, retromolar trigone.

<sup>c</sup>FOM, floor of mouth.

<sup>d</sup>Staging as per AJCC/UICC TNM 8th edition.

<sup>e</sup>No cN3a as per AJCC/UICC 8th edition TNM classification.

#### 4 | Discussion

At present, the prognostication of OSCC is solely based on the AJCC/UICC staging system [12]. However, tumors of the same stage do not behave similarly with respect to aggressiveness and response to therapy owing to their heterogeneity. In recent times, TME has certainly established itself as one of the prime areas of research. More so with the incorporation of immunotherapy in the cancer treatment guidelines. The effect of immune infiltration on carcinogenesis is varied and based on the class of immune cells and their spatial differential distribution within TME, making it a viable proposition for prognostic biomarker study. CD8<sup>+</sup> TILs are the most studied and validated among the whole spectrum of immune infiltrates [10, 11, 16–19]. Two recent systematic reviews and meta-analyses analyzed TILs, TAMs, and NK cells altogether in the prognostication of OSCC [10, 11]. Even after having majorly identical study designs and results, both studies cited a lack of reliability of the included studies, reporting irregularities and importantly, a minor effect on survival. CD8<sup>+</sup> cytotoxic TILs and CD57<sup>+</sup> NK cells are “anti-tumorigenic”, whereas FOXP3<sup>+</sup> T-regulatory cells and CD163<sup>+</sup> M2 macrophages are “pro-tumorigenic” [20]. High tumoral infiltration of CD8<sup>+</sup> TILs and CD57<sup>+</sup> NK cells has demonstrated a better clinical outcome. On the contrary, high infiltration of CD163<sup>+</sup> M2 macrophages was found to be associated with worse outcomes [10, 11]. Multiple studies have shown that a high CD8<sup>+</sup> expression was associated with negative regional metastasis [16, 21, 22]. Moreover, patients with abundant CD57<sup>+</sup> NK cells showed no regional metastasis and early clinical stage [21].

Our study differs from these findings as it failed to establish any strong correlation with any of the studied clinical and pathological prognostic variables. In a study by Troiano et al. [23] no association was found between CD68<sup>+</sup> TAM expression and lymph node metastasis, tumor stage, and histological grade. Similar results were obtained for the association of CD163<sup>+</sup> TAMs with lymph node metastasis and tumor stage. Kumar et al. [24] showed that a higher density of CD163<sup>+</sup> M2 macrophages in the tumor microenvironment is associated with advanced T-stage, increased rates of nodal positivity, and the presence of LVI. The same group of authors also concluded that there is no significant association between CD163 density and histological grade. The possible explanation of poor infiltration by FOXP3<sup>+</sup> TILs and CD57<sup>+</sup> NK cells may be due to unexplained interplay between advanced stage primaries (64% of pathological stage-IV tumors) and chemokine gradients, organization of extra-cellular matrix and collagen structure which are known barriers to immune infiltration [25]. We additionally studied CD45<sup>+</sup> pan-leukocytic tumor infiltration which was also majorly non-contributory. The probable protective effect of leukocytic infiltration on bone invasion was based on a subset analysis ( $n = 77$ ) and must be interpreted cautiously. Our study supports the findings of Troiano and colleagues, whereas majorly disagree with the other. All these studies have drawn their statistical conclusions based on 2×2 contingency tables. We chose Kendall's Tau and Rank-biserial correlations to additionally measure the direction and strength of the associations between variables. Though few of the immune markers attained statistical significance, none of the associations were strong enough to draw a valid conclusion

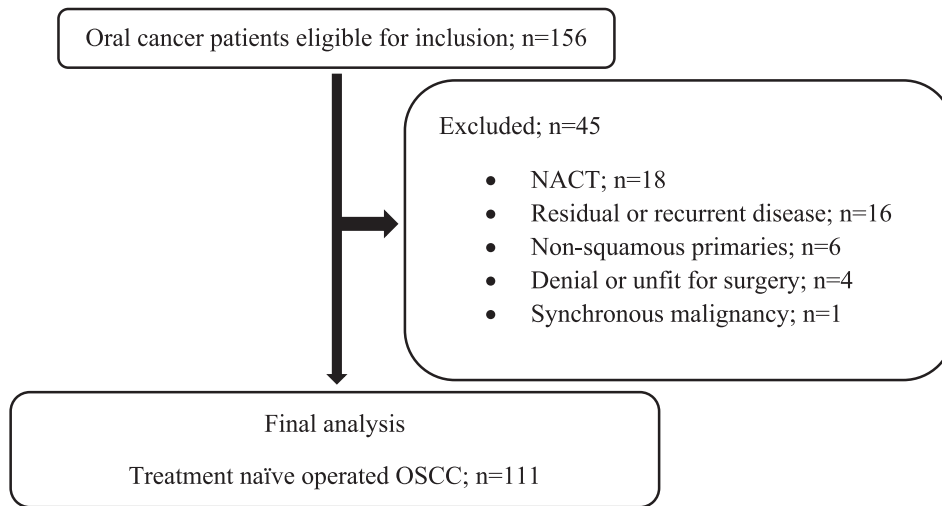


**FIGURE 1** | A flow diagram of the study.

**TABLE 2** | Distribution of HIDI score in the study cohort ( $n = 111$ ).

Immune cells	Median value (IQR)	Immune cells	Median value (IQR)
CD3 <sup>+</sup> TILs		CD68 <sup>+</sup> TAMs	
IM	9 (3)	IM	4 (8)
TC	6 (7)	TC	4 (5)
CD8 <sup>+</sup> TILs		CD163 <sup>+</sup> TAMs	
IM	6 (5)	IM	6 (8)
TC	3 (4)	TC	3 (8)
FOXP3 <sup>+</sup> TILs		CD45 <sup>+</sup> Leukocytes	
IM	1 (4)	IM	9 (3)
TC	1 (3)	TC	4 (5)
CD57 <sup>+</sup> NK cells			
IM	0 (1)		
TC	0 (1)		

(Table 2). The available literature also varied significantly in methodology and study reporting, hampering a direct comparison with the findings of the present study. We did not consider CD4<sup>+</sup> Memory T-lymphocytes as this subpopulation of TILs has an indirect influence on host protection by regulating the recruitment and activation of CD8<sup>+</sup> cytotoxic TILs [26].

The present study, to the best of our knowledge, is the only prospective study evaluating a comprehensive panel of tumor immune infiltrates in OSCC. Our study findings adhered to 16 out of 20 REMARK guidelines. We also partially adhered to the IIOB-WG recommendations. In fact, we believe, the incorporation of intensity to density scoring may add valuable functional information [27–29]. The proposed semiquantitative HIDI score is feasible, and reproducible, and does not require tedious manual counting of cells or specialized software support for whole slide image analysis. It also avoids the determination of high and low tumor infiltrates based on mean and median values used in most of the quantitative studies, which will always be dynamic

and vary between population and subsites [16–18, 29, 30]. The strong positive correlation between IM and TC compartments in our study can be interpreted in two ways. Firstly, the pattern of infiltration in the tumor core can be predicted by studying the invasive margin or vice versa. Secondly, adequate information may be generated just by studying a single compartment reducing the cost and time of analysis.

The present study failed to demonstrate any clinically significant correlation between immune infiltrates and other established clinical and pathological prognosticators in OSCC including the present AJCC/UICC staging system. Our study additionally addressed contemporary pathological variables like lymph node ratio (LNR) and lower neck metastases (level-IV/V), but it lacks a description of a few emerging evidence like tumor budding and WPOI-4. We also did not assess stromal TILs separately in the TC compartment due to the variability introduced by stromal desmoplasia which may act as a confounder and may not be generalized to other subsites in the head and neck, particularly

**TABLE 3** | Correlation of HID1 scores across all tumor-infiltrating immune cells ( $n = 111$ ; Kendall's tau-b statistics).

Immune cells	CD3 IM	CD3 TC	CD57 IM	CD57 TC	CD45 IM	CD45 TC	FOXP3 IM	FOXP3 TC	CD68 IM	CD68 TC	CD163 IM	CD163 TC	CD8 IM	CD8 TC
CD3 IM	—	<b>0.532</b> ; $p < 0.00001$	0.141; $p = 0.1$	0.169; $p = 0.05$	0.12; $p = 0.17$	0.055; $p = 0.5$	0.044; $p = 0.6$	0.07; $p = 0.4$	0.129; $p = 0.11$	0.138; $p = 0.09$	0.112; $p = 0.18$	0.2; $p = 0.01$	0.33; $p < 0.001$	0.329; $p < 0.001$
CD3 TC	<b>0.532</b> ; $p < 0.00001$	—	0.123; $p = 0.12$	0.138; $p = 0.09$	0.077; $p = 0.34$	0.115; $p = 0.13$	0.076; $p = 0.32$	0.092; $p = 0.24$	0.162; $p = 0.03$	0.188; $p = 0.01$	0.017; $p = 0.82$	0.085; $p = 0.27$	0.275; $p < 0.001$	0.389; $p < 0.001$
CD57 IM	0.141; $p = 0.1$	0.123; $p = 0.12$	—	<b>0.86</b> ; $p < 0.001$	0.038; $p = 0.65$	0.02; $p = 0.8$	−0.097; $p = 0.23$	−0.094; $p = 0.25$	0.155; $p = 0.05$	0.17; $p = 0.03$	0.158; $p = 0.05$	0.156; $p = 0.05$	0.153; $p = 0.06$	0.02; $p = 0.8$
CD57 TC	0.169; $p = 0.05$	0.138; $p = 0.09$	<b>0.86</b> ; $p < 0.00001$	—	0.06; $p = 0.48$	0.057; $p = 0.47$	−0.134; $p = 0.1$	−0.137; $p = 0.09$	0.165; $p = 0.04$	0.174; $p = 0.03$	0.126; $p = 0.13$	0.153; $p = 0.06$	0.169; $p = 0.04$	0.066; $p = 0.4$
CD45 IM	0.12; $p = 0.17$	0.077; $p = 0.34$	0.038; $p = 0.65$	0.06; $p = 0.48$	—	0.465; $p < 0.001$	0.284; $p < 0.001$	0.286; $p < 0.001$	0.098; $p = 0.22$	0.116; $p = 0.15$	−0.29; $p < 0.001$	−0.218; $p = 0.007$	0.116; $p = 0.16$	0.135; $p = 0.09$
CD45 TC	0.055; $p = 0.5$	0.115; $p = 0.13$	0.02; $p = 0.8$	0.057; $p = 0.47$	0.465; $p < 0.001$	—	0.144; $p = 0.6$	0.186; $p = 0.01$	0.124; $p = 0.1$	0.151; $p = 0.04$	−0.07; $p = 0.36$	−0.015; $p = 0.85$	0.124; $p = 0.1$	0.083; $p = 0.26$
FOXP3 IM	0.044; $p = 0.6$	0.076; $p = 0.32$	−0.097; $p = 0.23$	−0.134; $p = 0.1$	0.284; $p < 0.001$	0.144; $p = 0.6$	—	<b>0.904</b> ; $p < 0.00001$	−0.042; $p = 0.58$	−0.005; $p = 0.95$	−0.064; $p = 0.41$	−0.074; $p = 0.34$	0.069; $p = 0.38$	0.098; $p = 0.2$
FOXP3 TC	0.07; $p = 0.4$	0.092; $p = 0.24$	−0.094; $p = 0.25$	−0.137; $p = 0.09$	0.286; $p < 0.001$	0.186; $p = 0.01$	<b>0.904</b> ; $p < 0.00001$	—	−0.049; $p = 0.53$	−0.009; $p = 0.9$	−0.046; $p = 0.56$	−0.062; $p = 0.43$	0.102; $p = 0.2$	0.124; $p = 0.11$
CD68 IM	0.129; $p = 0.11$	0.162; $p = 0.03$	0.155; $p = 0.05$	0.165; $p = 0.04$	0.098; $p = 0.22$	0.124; $p = 0.1$	−0.042; $p = 0.58$	−0.049; $p = 0.53$	—	<b>0.916</b> ; $p < 0.00001$	−0.103; $p = 0.18$	−0.045; $p = 0.55$	0.1; $p = 0.19$	0.167; $p = 0.03$
CD68 TC	0.138; $p = 0.09$	0.188; $p = 0.01$	0.17; $p = 0.03$	0.174; $p = 0.03$	0.116; $p = 0.15$	0.151; $p = 0.04$	−0.005; $p = 0.95$	−0.009; $p = 0.9$	<b>0.916</b> ; $p < 0.00001$	—	−0.082; $p = 0.29$	−0.025; $p = 0.74$	0.077; $p = 0.31$	0.159; $p = 0.03$
CD163 IM	0.112; $p = 0.18$	0.017; $p = 0.82$	0.158; $p = 0.05$	0.126; $p = 0.13$	−0.29; $p < 0.001$	−0.07; $p = 0.36$	—	−0.082; $p = 0.29$	−0.103; $p = 0.18$	−0.082; $p = 0.29$	—	<b>0.852</b> ; $p < 0.00001$	−0.026; $p = 0.75$	−0.086; $p = 0.26$
CD163 TC	0.2; $p = 0.01$	0.085; $p = 0.27$	0.156; $p = 0.05$	0.153; $p = 0.06$	0.155; $p = 0.05$	0.156; $p = 0.05$	0.158; $p = 0.05$	0.156; $p = 0.05$	0.155; $p = 0.05$	0.17; $p = 0.03$	0.158; $p = 0.05$	0.156; $p = 0.05$	0.153; $p = 0.06$	0.02; $p = 0.8$
CD8 IM	0.33; $p < 0.001$	0.275; $p < 0.001$	0.153; $p = 0.06$	0.169; $p = 0.04$	0.116; $p = 0.16$	0.124; $p = 0.1$	0.069; $p = 0.38$	0.102; $p = 0.2$	0.1; $p = 0.19$	0.077; $p = 0.31$	−0.026; $p = 0.75$	0.003; $p = 0.97$	—	<b>0.602</b> ; $p < 0.00001$
CD8 TC	0.329; $p < 0.001$	0.389; $p < 0.001$	0.02; $p = 0.8$	0.066; $p = 0.4$	0.135; $p = 0.09$	0.083; $p = 0.26$	0.098; $p = 0.2$	0.124; $p = 0.11$	0.167; $p = 0.03$	0.159; $p = 0.03$	−0.086; $p = 0.26$	−0.011; $p = 0.89$	<b>0.602</b> ; $p < 0.00001$	—

Note: Significant correlations (moderately strong upwards) are highlighted in **bold**; p-values are adjusted to Bonferroni correction ( $p < 0.00027$  statistically significant).

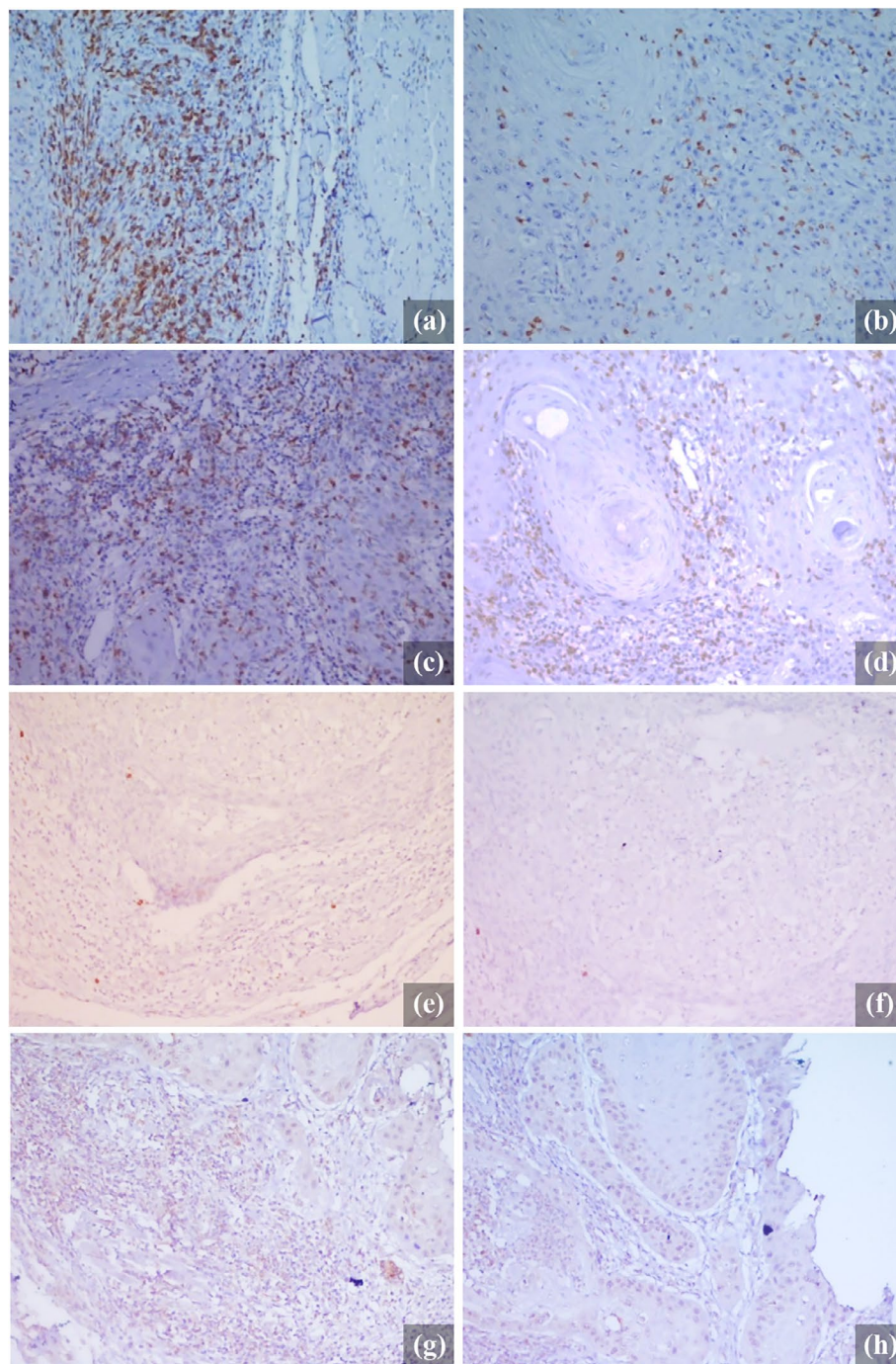


**FIGURE 2** | The representative immunohistochemistry images show the spatial distribution and density of various tumor immune infiltrates in the study population. (a) CD3<sup>+</sup> TILs in tumor invasive margin (CD3-IM); (b) CD3<sup>+</sup> TILs in tumor core (CD3-TC); (c) CD8-IM; (d) CD8-TC; (e) CD57-IM; (f) CD57-TC; (g) CD68-IM; (h) CD68-TC; (i) CD163-IM; (j) CD163-TC; (k) FOXP3-IM; (l) FOXP3-TC; (m) CD45-IM; (n) CD45-TC. [Color figure can be viewed at [wileyonlinelibrary.com](http://wileyonlinelibrary.com)]

oropharynx and lymph nodes [14]. The present study lacks survival statistics too, which are required to validate our findings. A multivariate analysis along with an attempt to stratify the HIDI score based on survival statistics is planned in subsequent publications in due course.

However, the present study unfolds multiple hypotheses which may guide future research in this regard. Firstly, whether the tumor immune infiltrates have an independent effect on survival

is supported by the published literature [10–11, 16–19, 23–24, 29–31]. Secondly, whether high versus low immune infiltration has any significant prognostic difference. We noticed very low tumor infiltration by CD57<sup>+</sup> NK cells in our cohort. Whereas the existing evidence suggests high infiltration of CD57<sup>+</sup> NK cells improves overall survival [10, 11, 16]. Thirdly, CD3<sup>+</sup> and CD8<sup>+</sup> TILs may be the target of choice for immunotherapy with the highest tumoral infiltration as demonstrated in the study. Fourthly, whether the incorporation of immune infiltrates in the

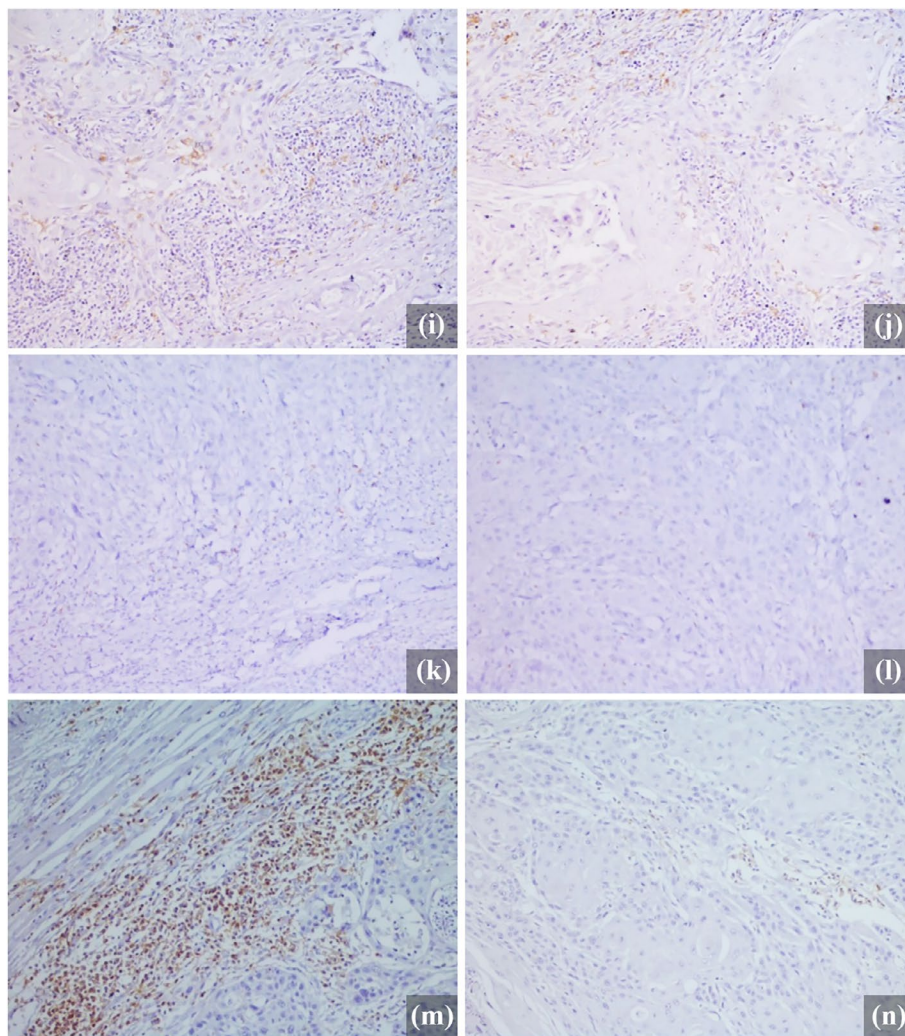


**FIGURE 2** | (Continued)

**TABLE 4** | Significant correlation statistics of tumor immune infiltrates with clinical and pathological variables ( $n = 111$ ).

Correlation statistics	Primary characteristics	Immune cells	Complementary characteristics	Correlation statistics
$\tau b^a = -0.153; p = 0.04$ $\tau b = -0.147; p = 0.05$	Age	CD57 IM CD57 TC	N.A.	N.A. <sup>c</sup>
$\tau b = 0.206; p = 0.01$ $\tau b = -0.193; p = 0.022$	cT classification	CD45 TC CD57 IM	pT classification	N.S. <sup>d</sup> $\tau b = -0.172; p = 0.038$
$\tau b = 0.174; p = 0.036$ $\tau b = 0.167; p = 0.031$ $\tau b = 0.196; p = 0.012$ $\tau b = 0.212; p = 0.006$	cN classification	CD45 IM CD45 TC CD68 IM CD68 TC	pN classification	N.S. N.S. N.S. $\tau b = 0.158; p = 0.043$
$\tau b = 0.181; p = 0.027$ $\tau b = 0.169; p = 0.038$	Clinical stage	CD68 IM CD68 TC	Pathological stage	N.S. N.S.
$r_{rb}^b = -0.351; p = 0.002$	Bony invasion	CD45 IM	N.A.	N.A.
$r_{rb} = -0.21; p = 0.027$	LVI	CD57 TC	N.A.	N.A.
$\tau b = 0.266; p = 0.029$	ENE	CD57 TC	N.A.	N.A.

<sup>a</sup> $\tau b$ , Kendall's tau-b statistic.

<sup>b</sup> $r_{rb}$ , Rank-Biserial statistic.

<sup>c</sup>N.A., not applicable.

<sup>d</sup>N.S., not significant.

existing TNM classification (iTNM) improves the predictive accuracy of the present staging system in OSCC requires further research [32]. Similar additional measures are routinely practiced for oropharyngeal (p16/HPV) [12, 33, 34], breast (ER/PR/HER2Neu) [35, 36], and colorectal (MSI) [37–39] cancers and carry tremendous prognostic values. The inclusion of the entire spectrum of TILs, TAMs, and NK cells is suggested to determine their true prognostic potential. As none of the methodologies are validated on a large scale to date, compliance with REMARK and IIOB-WG recommendations is strictly encouraged.

## Author Contributions

R.K.S., A.S.: conceptualization, data curation, formal analysis, methodology, project administration, resources, software, supervision, visualization, roles/writing – original draft, and writing – review and editing. V.N.G.: data curation, methodology; formal analysis, visualization, roles/writing – review and editing. D.R.P.: conceptualization, formal analysis, methodology, supervision, roles/writing – review and editing. K.S.M.: conceptualization, data curation, formal analysis, methodology, project administration, resources, software, supervision, visualization, roles/writing – original draft, and writing – review and editing. T.A., P.K., A.P., V.S.K., R.K.: data curation, methodology, visualization, roles/writing – review and editing. N.C.: data curation, methodology, software, roles/writing – review and editing.

## Acknowledgments

The authors acknowledge all the technical and non-technical staff of the Departments of Surgical Oncology and Pathology, All India Institute of Medical Sciences, Rishikesh, India for their support in printing documents and retrieving histopathology blocks for immunohistochemistry.

## Ethics Statement

The study protocol was reviewed and approved by the institutional ethics committee (ECR/736/Inst/UK/2015/RR-18), approval no. AIIMS/IEC/20/409 dated June 20, 2020.

## Consent

Written informed consents were obtained from each study participant.

## Conflicts of Interest

The authors declare no conflicts of interest.

## Data Availability Statement

The data that support the findings of this study are available from the corresponding author, [K.S.M.], upon reasonable request.

## References

1. D. Hanahan and R. A. Weinberg, “The Hallmarks of Cancer,” *Cell* 100, no. 1 (January 2000): 57–70, [https://doi.org/10.1016/s0092-8674\(00\)81683-9](https://doi.org/10.1016/s0092-8674(00)81683-9).
2. D. Hanahan and R. A. Weinberg, “Hallmarks of Cancer: The Next Generation,” *Cell* 144, no. 5 (March 2011): 646–674, <https://doi.org/10.1016/j.cell.2011.02.013>.
3. H. Ujiie, K. Kadota, J. I. Nitadori, et al., “The Tumoral and Stromal Immune Microenvironment in Malignant Pleural Mesothelioma: A Comprehensive Analysis Reveals Prognostic Immune Markers,”

*Oncoimmunology* 4, no. 6 (March 2015): e1009285, <https://doi.org/10.1080/2162402X.2015.1009285>.

4. S. Punt, E. A. Dronkers, M. J. Welters, et al., “A Beneficial Tumor Microenvironment in Oropharyngeal Squamous Cell Carcinoma Is Characterized by a High T Cell and Low IL-17(+) Cell Frequency,” *Cancer Immunology, Immunotherapy* 65, no. 4 (April 2016): 393–403, <https://doi.org/10.1007/s00262-016-1805-x>.

5. J. Galon, B. Mlecnik, G. Bindea, et al., “Towards the Introduction of the ‘Immunoscore’ in the Classification of Malignant Tumours,” *Journal of Pathology* 232, no. 2 (January 2014): 199–209, <https://doi.org/10.1002/path.4287>.

6. A. Kirilovsky, F. Marliot, C. El Sissy, N. Haicheur, J. Galon, and F. Pagès, “Rational Bases for the Use of the Immunoscore in Routine Clinical Settings as a Prognostic and Predictive Biomarker in Cancer Patients,” *International Immunology* 28, no. 8 (August 2016): 373–382, <https://doi.org/10.1093/intimm/dxw021>.

7. R. Salgado, C. Denkert, S. Demaria, et al., “The Evaluation of Tumor-Infiltrating Lymphocytes (TILs) in Breast Cancer: Recommendations by an International TILs Working Group 2014,” *Annals of Oncology* 26, no. 2 (2015): 259–271, <https://doi.org/10.1093/annonc/mdl450>.

8. T. Donnem, T. K. Kilvaer, S. Andersen, et al., “Strategies for Clinical Implementation of TNM-Immunoscore in Resected Non-small-Cell Lung Cancer,” *Annals of Oncology* 27, no. 2 (February 2016): 225–232, <https://doi.org/10.1093/annonc/mdv560>.

9. A. De Meulenaere, T. Vermassen, S. Aspeslagh, K. Vandecasteele, S. Rottey, and L. Ferdinande, “TILs in Head and Neck Cancer: Ready for Clinical Implementation and Why (Not)?,” *Head and Neck Pathology* 11, no. 3 (September 2017): 354–363, <https://doi.org/10.1007/s12105-016-0776-8>.

10. Z. Huang, N. Xie, H. Liu, et al., “The Prognostic Role of Tumour-Infiltrating Lymphocytes in Oral Squamous Cell Carcinoma: A Meta-Analysis,” *Journal of Oral Pathology & Medicine* 48, no. 9 (October 2019): 788–798, <https://doi.org/10.1111/jop.12927>.

11. E. Hadler-Olsen and A. M. Wirsing, “Tissue-Infiltrating Immune Cells as Prognostic Markers in Oral Squamous Cell Carcinoma: A Systematic Review and Meta-Analysis,” *British Journal of Cancer* 120, no. 7 (April 2019): 714–727, <https://doi.org/10.1038/s41416-019-0409-6>.

12. M. B. Amin, F. L. Greene, S. B. Edge, et al., “The Eighth Edition AJCC Cancer Staging Manual: Continuing to Build a Bridge From a Population-Based to a More “Personalized” Approach to Cancer Staging,” *CA: A Cancer Journal for Clinicians* 67, no. 2 (March 2017): 93–99, <https://doi.org/10.3322/caac.21388>.

13. L. M. McShane, D. G. Altman, W. Sauerbrei, S. E. Taube, M. Gion, and G. M. Clark, “Statistics Subcommittee of the NCI-EORTC Working Group on Cancer Diagnostics. REporting Recommendations for Tumour MARKer Prognostic Studies (REMARK),” *British Journal of Cancer* 93, no. 4 (August 2005): 387–391, <https://doi.org/10.1038/sj.bjc.6602678>.

14. S. Hendry, R. Salgado, T. Gevaert, et al., “Assessing Tumor-Infiltrating Lymphocytes in Solid Tumors: A Practical Review for Pathologists and Proposal for a Standardized Method From the International Immunology Biomarkers Working Group: Part 2: TILs in Melanoma, Gastrointestinal Tract Carcinomas, Non-Small Cell Lung Carcinoma and Mesothelioma, Endometrial and Ovarian Carcinomas, Squamous Cell Carcinoma of the Head and Neck, Genitourinary Carcinomas, and Primary Brain Tumors,” *Advances in Anatomic Pathology* 24, no. 6 (November 2017): 311–335, <https://doi.org/10.1097/PAP.0000000000000161>.

15. N. Subramaniam, D. Balasubramanian, N. Kumar, et al., “Lymph Node Staging Systems in Oral Squamous Cell Carcinoma: A Comparative Analysis,” *Oral Oncology* 97 (October 2019): 92–98, <https://doi.org/10.1016/j.oraloncology.2019.08.002>.

16. J. Fang, X. Li, D. Ma, et al., “Prognostic Significance of Tumor Infiltrating Immune Cells in Oral Squamous Cell Carcinoma,” *BMC Cancer* 17, no. 1 (May 2017): 375, <https://doi.org/10.1186/s12885-017-3317-2>.

17. W. Y. Chen, C. T. Wu, C. W. Wang, et al., "Prognostic Significance of Tumor-Infiltrating Lymphocytes in Patients With Operable Tongue Cancer," *Radiation Oncology* 13, no. 1 (August 2018): 157, <https://doi.org/10.1186/s13014-018-1099-6>.
18. C. Zhou, Y. Wu, L. Jiang, et al., "Density and Location of CD3+ and CD8+ Tumor-Infiltrating Lymphocytes Correlate With Prognosis of Oral Squamous Cell Carcinoma," *Journal of Oral Pathology & Medicine* 47, no. 4 (April 2018): 359–367, <https://doi.org/10.1111/jop.12698>.
19. M. E. Spector, E. Bellile, L. Amlani, et al., "University of Michigan Head and Neck SPORE Program. Prognostic Value of Tumor-Infiltrating Lymphocytes in Head and Neck Squamous Cell Carcinoma," *JAMA Otolaryngology. Head & Neck Surgery* 145, no. 11 (November 2019): 1012–1019, <https://doi.org/10.1001/jamaoto.2019.2427>.
20. S. T. Paijens, A. Vledder, M. de Bruyn, and H. W. Nijman, "Tumor-Infiltrating Lymphocytes in the Immunotherapy Era," *Cellular & Molecular Immunology* 18, no. 4 (April 2021): 842–859, <https://doi.org/10.1038/s41423-020-00565-9>.
21. Y. A. Cho, H. J. Yoon, J. I. Lee, S. P. Hong, and S. D. Hong, "Relationship Between the Expressions of PD-L1 and Tumor-Infiltrating Lymphocytes in Oral Squamous Cell Carcinoma," *Oral Oncology* 47, no. 12 (December 2011): 1148–1153, <https://doi.org/10.1016/j.oraloncology.2011.08.007>.
22. P. Balernmpas, Y. Michel, J. Wagenblast, et al., "Tumour-Infiltrating Lymphocytes Predict Response to Definitive Chemoradiotherapy in Head and Neck Cancer," *British Journal of Cancer* 110, no. 2 (January 2014): 501–509, <https://doi.org/10.1038/bjc.2013.640>.
23. G. Troiano, V. C. A. Caponio, I. Adipietro, et al., "Prognostic Significance of CD68+ and CD163+ Tumor Associated Macrophages in Head and Neck Squamous Cell Carcinoma: A Systematic Review and Meta-Analysis," *Oral Oncology* 93 (June 2019): 66–75, <https://doi.org/10.1016/j.oraloncology.2019.04.019>.
24. A. T. Kumar, A. Knops, B. Swendseid, et al., "Prognostic Significance of Tumor-Associated Macrophage Content in Head and Neck Squamous Cell Carcinoma: A Meta-Analysis," *Frontiers in Oncology* 23, no. 9 (July 2019): 656, <https://doi.org/10.3389/fonc.2019.00656>.
25. M. M. Melssen, N. D. Sheybani, K. M. Leick, and C. L. Slingluff, Jr., "Barriers to Immune Cell Infiltration in Tumors," *Journal for Immunotherapy of Cancer* 11, no. 4 (April 2023): e006401, <https://doi.org/10.1136/jitc-2022-006401>.
26. J. dos antos Pereira, M. C. da Costa Miguel, L. M. Guedes Queiroz, and É. J. da Silveira, "Analysis of CD8+ and CD4+ Cells in Oral Squamous Cell Carcinoma and Their Association With Lymph Node Metastasis and Histologic Grade of Malignancy," *Applied Immunohistochemistry & Molecular Morphology* 22, no. 3 (March 2014): 200–205, <https://doi.org/10.1097/PAI.0b013e31828df3c9>.
27. S. Umemura, M. Kurosumi, T. Moriya, et al., "Immunohistochemical Evaluation for Hormone Receptors in Breast Cancer: A Practically Useful Evaluation System and Handling Protocol," *Breast Cancer* 13, no. 3 (2006): 232–235, <https://doi.org/10.2325/jbcs.13.232>.
28. S. W. Kim, J. Roh, and C. S. Park, "Immunohistochemistry for Pathologists: Protocols, Pitfalls, and Tips," *Journal of Pathology and Translational Medicine* 50, no. 6 (November 2016): 411–418, <https://doi.org/10.4132/jptm.2016.08.08>.
29. P. Lequerica-Fernández, J. Suárez-Canto, T. Rodríguez-Santamarta, et al., "Prognostic Relevance of CD4+, CD8+ and FOXP3+ TILs in Oral Squamous Cell Carcinoma and Correlations With PD-L1 and Cancer Stem Cell Markers," *Biomedicine* 9, no. 6 (June 2021): 653, <https://doi.org/10.3390/biomedicine9060653>.
30. X. M. Zhang, L. J. Song, J. Shen, et al., "Prognostic and Predictive Values of Immune Infiltrate in Patients With Head and Neck Squamous Cell Carcinoma," *Human Pathology* 82 (December 2018): 104–112, <https://doi.org/10.1016/j.humpath.2018.07.012>.
31. J. H. Cho and Y. C. Lim, "Prognostic Impact of Regulatory T Cell in Head and Neck Squamous Cell Carcinoma: A Systematic Review and Meta-Analysis," *Oral Oncology* 112 (January 2021): 105084, <https://doi.org/10.1016/j.oraloncology.2020.105084>.
32. U. S. Vishal Rao, S. S. Shetty, A. Kudpaje, G. A. Rao, and S. S. Kuniyal, "A TNM Staging for Head and Neck Cancers," *Oral Oncology* 97 (October 2019): 133–134, <https://doi.org/10.1016/j.oraloncology.2019.08.016>.
33. K. K. Ang, J. Harris, R. Wheeler, et al., "Human Papillomavirus and Survival of Patients With Oropharyngeal Cancer," *New England Journal of Medicine* 363, no. 1 (July 2010): 24–35, <https://doi.org/10.1056/NEJMoa0912217>.
34. C. Fakhry, C. Lacchetti, L. M. Rooper, et al., "Human Papillomavirus Testing in Head and Neck Carcinomas: ASCO Clinical Practice Guideline Endorsement of the College of American Pathologists Guideline," *Journal of Clinical Oncology* 36, no. 31 (November 2018): 3152–3161, <https://doi.org/10.1200/JCO.18.00684>.
35. K. H. Allison, M. E. H. Hammond, M. Dowsett, et al., "Estrogen and Progesterone Receptor Testing in Breast Cancer: ASCO/CAP Guideline Update," *Journal of Clinical Oncology* 38, no. 12 (April 2020): 1346–1366, <https://doi.org/10.1200/JCO.19.02309>.
36. A. C. Wolff, M. R. Somerfield, M. Dowsett, et al., "Human Epidermal Growth Factor Receptor 2 Testing in Breast Cancer: ASCO-College of American Pathologists Guideline Update," *Journal of Clinical Oncology* 41, no. 22 (August 2023): 3867–3872, <https://doi.org/10.1200/JCO.22.02864>.
37. C. R. Boland and A. Goel, "Microsatellite Instability in Colorectal Cancer," *Gastroenterology* 138, no. 6 (June 2010): 2073–2087.e3, <https://doi.org/10.1053/j.gastro.2009.12.064>.
38. K. Li, H. Luo, L. Huang, H. Luo, and X. Zhu, "Microsatellite Instability: A Review of What the Oncologist Should Know," *Cancer Cell International* 13, no. 20 (January 2020): 16, <https://doi.org/10.1186/s12935-019-1091-8>.
39. V. K. Morris, E. B. Kennedy, N. N. Baxter, et al., "Treatment of Metastatic Colorectal Cancer: ASCO Guideline," *Journal of Clinical Oncology* 41, no. 3 (January 2023): 678–700, <https://doi.org/10.1200/JCO.22.01690>.

## Supporting Information

Additional supporting information can be found online in the Supporting Information section.